

# Closed-Loop Recycling of Mixed Plastics of Polyester and CO<sub>2</sub>-Based Polycarbonate to a Single Monomer

Changxia Shi, Wilfred T. Diment, and Eugene Y.-X. Chen\*

**Abstract:** Physical blending is an effective strategy for tailoring polymeric materials to specific application requirements. However, physically blended mixed plastics waste adds additional barriers in mechanical or chemical recycling. This difficulty arises from the intricate requirement for meticulous sorting and separation of the various polymers in the inherent incompatibility of mixed polymers during recycling. To overcome this impediment, this work furthers the emerging single-monomer – multiple-materials approach through the design of a bifunctional monomer that can not only orthogonally polymerize into two different types of polymers – specifically lactone-based polyester and CO<sub>2</sub>-based polycarbonate – but the resultant polymers and their mixture can also be depolymerized back to the single, original monomer when facilitated by catalysis. Specifically, the lactone/epoxide hybrid bifunctional monomer (BiL<sup>O</sup>) undergoes ring-opening polymerization through the lactone manifold to produce polyester, PE(BiL<sup>O</sup>), and is also applied to ring-opening copolymerization with CO<sub>2</sub>, via the epoxide manifold, to yield polycarbonate, PC(BiL<sup>O</sup>). Remarkably, a one-pot recycling process of a BiL<sup>O</sup>-derived PE/PC blend back to the constituent monomer BiL<sup>O</sup> in >99% selectivity was achieved with a superbase catalyst at 150 °C, thereby effectively obviating the requirement for sorting and separation typically required for recycling of mixed polymers.

mers, this closed-loop chemical recycling represents an advantage over mechanical recycling methods, which typically result in materials with diminished properties.<sup>[2]</sup> Much of the work on chemical recycling focuses on selective depolymerization of single-material streams.<sup>[3]</sup> However, real-world plastic products often comprise mixed plastics with varied chemical structures, tailored to meet specific application needs.<sup>[4]</sup> This complexity presents significant challenges in the separation processes required to isolate individual polymers for recycling, leading to escalated costs and limiting the feasibility of large-scale chemical recycling from both operational and economic viewpoints.<sup>[5]</sup> Upcycling mixed plastics into value-added products offers an alternative approach that could bypass this limitation and substantially enhance plastics reclamation. However, this method represents an open-loop recycling process which, while beneficial, falls short of establishing a true circular economy for plastics.<sup>[6]</sup> The above overview highlights a pressing need for developing effective methods to enable the closed-loop recycling of mixed plastics, thereby negating the need for meticulous sorting.

Addressing this challenge calls for more than just innovative recycling technologies; it also demands a fundamental paradigm shift towards a mindset focused on circularity. A sustainable path forward involves transitioning from finite, fossil-based resources to renewable, abundant alternatives. In this context, harnessing and converting CO<sub>2</sub> as a renewable resource holds significant potential.<sup>[7]</sup> For instance, the ring-opening copolymerization (ROCOP) of CO<sub>2</sub> with epoxides to produce degradable aliphatic polycarbonates (PCs) represents a promising avenue for large-scale utilization of CO<sub>2</sub> as a renewable C1 feedstock.<sup>[8]</sup> Chemical recycling of CO<sub>2</sub>-based PCs back to constituent epoxides provides a route towards establishing a circular economy for CO<sub>2</sub>-based PCs. While there are various structures of epoxides that can be utilized to produce PCs with CO<sub>2</sub>, truly closed-loop recyclable examples are currently largely limited to specific structures such as cyclopentene oxide, cyclohexene oxide (CHO), limonene 1,2-monoxide and nitrogen-containing epoxides.<sup>[9]</sup> The main obstacle for achieving chemical recycling of CO<sub>2</sub>-based PCs is the formation of thermodynamically stable five-membered cyclic carbonates, which resist repolymerization.<sup>[10]</sup>

Poly(cyclohexene carbonate) (PCHC), synthesized from the copolymerization of CHO and CO<sub>2</sub>, has attracted significant interest as a potential sustainable engineering plastic due to its notable tensile strength and high glass transition temperature (*T<sub>g</sub>*).<sup>[8a]</sup> However, the chemical recycling of PCHC back to CHO has long been a challeng-

## Introduction

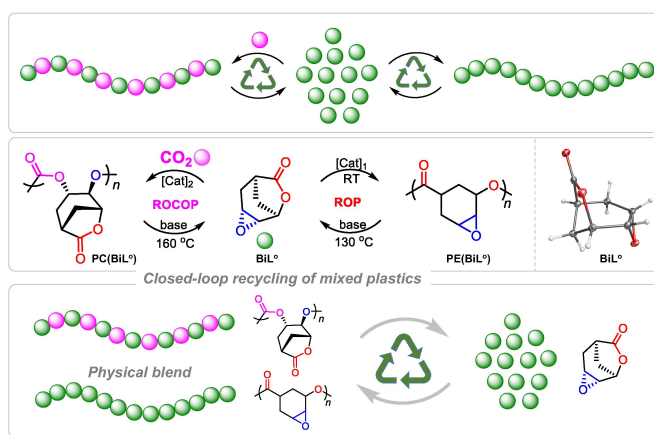
The chemical recycling of end-of-life (EoL) polymers back to their constituent monomers presents a promising solution to the EoL issue of plastic waste, paving the way for achieving a circular plastic economy.<sup>[1]</sup> As the recovered monomers can be repolymerized into virgin-quality poly-

[\*] Dr. C. Shi, Dr. W. T. Diment, Prof. Dr. E. Y.-X. Chen  
 Department of Chemistry, Colorado State University  
 Fort Collins, Colorado 80523-1872, United States  
 E-mail: eugene.chen@colostate.edu

© 2024 The Author(s). Angewandte Chemie International Edition published by Wiley-VCH GmbH. This is an open access article under the terms of the Creative Commons Attribution Non-Commercial License, which permits use, distribution and reproduction in any medium, provided the original work is properly cited and is not used for commercial purposes.

ing endeavor, attributed to the fact that *trans*-cyclohexene carbonate (*trans*-CHC) is a more thermodynamically favored depolymerization product than CHO itself.<sup>[11]</sup> Despite these difficulties, several recent reports have detailed the efficient chemical recycling of PCHC back to CHO. Notably, in 2022, Williams and Zhang independently demonstrated the selective depolymerization of PCHC to CHO in toluene, using a homodinuclear magnesium(II) complex and a heterogeneous multinuclear zinc catalysts, respectively.<sup>[12]</sup> In a further breakthrough, Liu and Lu uncovered that a Cr<sup>III</sup>-Salen complex coupling with PPNN<sub>3</sub> cocatalyst, was able to quantitatively convert PCHC into CHO in bulk.<sup>[13]</sup> More recently, Williams and co-workers made significant progress in the bulk depolymerization of various aliphatic PCs, including PCHC, by utilizing a heterodinuclear Mg<sup>II</sup>-Co<sup>II</sup> catalyst.<sup>[14]</sup>

Given that plastic products typically comprise diverse materials to fulfill different performance criteria, their recycling and reuse present a formidable challenge, involving the need for laborious separation and purification procedures. These hurdles diminish the economic feasibility and hinder the broad adoption of plastic recycling.<sup>[15]</sup> Although several notable studies have successfully demonstrated that a target polymer can be effectively recycled back to its constituent monomers from mixed plastic streams,<sup>[14a,5a,16]</sup> the lack of EoL option for the remaining unrecyclable polymers in such mixed streams renders this approach less desirable.<sup>[3d]</sup> We have recently reported several efforts to develop closed-loop chemically recyclable polymers with “one monomer-two polymers-one monomer” features via a hybrid monomer design strategy.<sup>[1a,17]</sup> For example, a bicyclic lactone/olefin bifunctional monomer (BiL<sup>o</sup>), encompassing low ceiling temperature (*T<sub>c</sub>*) substructures of  $\gamma$ -butyrolactone toward ring-opening polymerization (ROP) and cyclohexene toward ring-opening metathesis polymerization, not only facilitated the efficient polymerization of the “nonpolymerizable” parent monomers but also provided orthogonal mechanistic pathways to generate two polymers with distinct material properties and full chemical recyclability to the same monomer.<sup>[17d]</sup> Notably, their physical blend can also be sequentially depolymerized back to their constituent monomer (BiL<sup>o</sup>). However, this recycling Scheme requires the use of different catalysts in two sequential steps. In addition to the need to address this problem, the scope of polymer classes that can be recycled from their mixtures in a closed-loop fashion must be explored and expanded. Herein, we report the selective generation of either polyester PE(BiL<sup>o</sup>) or polycarbonate PC(BiL<sup>o</sup>) from a bifunctional lactone/epoxide hybrid monomer (BiL<sup>o</sup>) via ROP or ROCOP with CO<sub>2</sub>. Importantly, both polymers and their mixture (blend) can be selectively depolymerized back to the same monomer BiL<sup>o</sup> (Scheme 1). This work serves as a striking demonstration of how two different types of polymers, derived from orthogonal polymerization of a single monomer, and their physical blend, can be selectively recycled back to the same monomer using commercially available catalysts.



**Scheme 1.** Schematic illustration of orthogonal polymerization of a bifunctional lactone/epoxide hybrid monomer (BiL<sup>o</sup>) into polyester via ROP and CO<sub>2</sub>-based PC via ROCOP and selective depolymerization of both polymers and their mixture back to BiL<sup>o</sup>, thus closing the circular loop in recycling mixed polymers.

## Results and Discussion

Monomer BiL<sup>o</sup> (Figure S1 and S2) was synthesized by the Baeyer–Villiger oxidation of 6-oxabicyclo[3.2.1]oct-3-en-7-one (BiL<sup>o</sup>) with *m*-CPBA, and was obtained in a relatively high overall isolated yield ~80%.<sup>[18]</sup> The molecular structure of the monomer was characterized by single crystal X-ray diffraction analysis (Scheme 1, inset, Table S4). The two functional groups present in BiL<sup>o</sup> offer the opportunity to create a wide range of polymer materials through the orthogonal polymerization pathways of these moieties. Specifically, the lactone manifold is designed to produce closed-loop circular polyester PE(BiL<sup>o</sup>) with CHO incorporated into the main chain rendering high-performance properties. On the other hand, the epoxide manifold presents a versatile platform for either homopolymerization to polyether or copolymerization with CO<sub>2</sub> to polycarbonate PC(BiL<sup>o</sup>).

### The Lactone Manifold to Produce Polyester PE(BiL<sup>o</sup>) via ROP

At the outset, we conducted a screening for the ROP of BiL<sup>o</sup> using both organocatalyst 1,5,7-triazabicyclo[4.4.0]dec-5-ene (TBD)<sup>[19]</sup> and metal-based catalyst La[N(SiMe<sub>3</sub>)<sub>2</sub>]<sub>3</sub> (La-1)<sup>[3a]</sup> (Figure 1A). The TBD-catalyzed ROP in CH<sub>2</sub>Cl<sub>2</sub> (6.0 M) at room temperature (RT, ~23 °C) with a [BiL<sup>o</sup>]/[TBD]/[BnOH] ratio of 100:1:1 (BnOH = benzyl alcohol, as the initiator) achieved 78 % conversion after 15 h, affording PE(BiL<sup>o</sup>) with a low number-average molar mass (*M<sub>n</sub>*) of 11.4 kg mol<sup>-1</sup> and a dispersity (*D*) of 1.38 (Table S1, run 1, Figure S3 and S4). Further exploring the ROP with [BiL<sup>o</sup>]/[TBD]/[BnOH] = 1000:2:1 in CH<sub>2</sub>Cl<sub>2</sub> (6.0 M) at RT, resulted in a monomer conversion of 50 % after 72 h, yielding P(BiL<sup>o</sup>)<sub>ROP</sub> with high *M<sub>n</sub>* = 55.3 kg mol<sup>-1</sup> and *D* = 1.33 (Table S1, run 2). Upon switching to metal-catalyzed coordinative-insertion ROP, the La-1 catalyzed

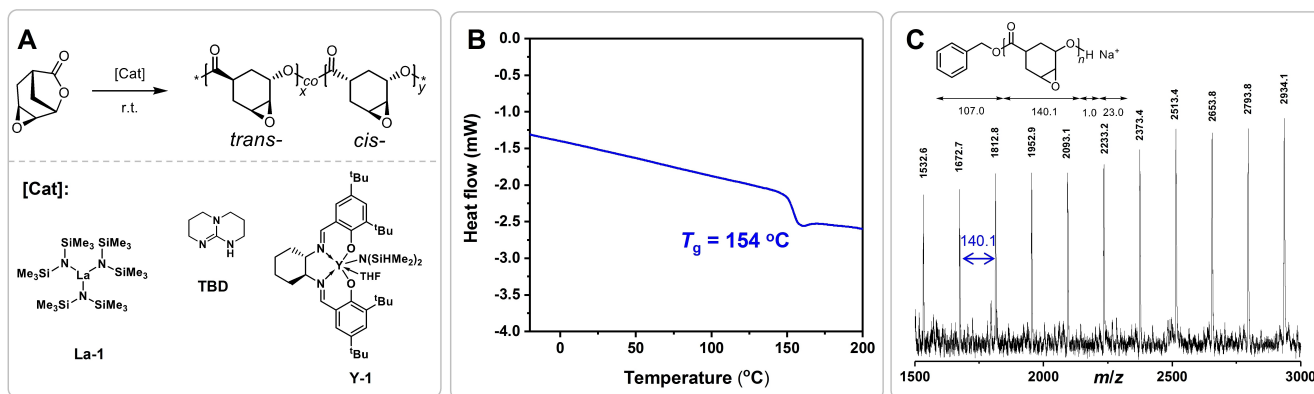


**Figure 1.** (A) ROP of BiL<sup>O</sup> catalyzed by various catalysts. (B) DSC curve for PE(BiL<sup>O</sup>) produced by La-1. (C) MALDI-TOF MS spectrum PE(BiL<sup>O</sup>) produced by TBD and BnOH.

polymerization achieved 58% conversion after 36 h with  $[\text{BiL}^{\text{O}}]/[\text{La-1}]/[\text{BnOH}] = 300:1:3$  (RT, 6.0 M in  $\text{CH}_2\text{Cl}_2$ ) (Table S1, run 3). Notably,  $^1\text{H}$  NMR spectrum of the PE(BiL<sup>O</sup>) produced by TBD revealed epimerization at the stereogenic carbon center adjacent to the carbonyl carbon, thus affording PE(BiL<sup>O</sup>) containing both *cis*- (50%) and *trans*- (50%) stereoconfigurations. In contrast, the PE(BiL<sup>O</sup>) prepared by La-1 is devoid of any detectable epimerization, as evidenced by the absence of the peaks associated with the *trans*-configuration in its  $^1\text{H}$  NMR spectrum (Figure S3 vs S5). The employment of a discrete yttrium complex supported by a  $C_2$ -symmetric Salen ligand (Y-1, Figure 1A), resulted in a higher  $M_n$  of  $77.4 \text{ kg mol}^{-1}$  (Table S1, run 5). Nevertheless, this approach did not completely suppress epimerization, yielding a polyester with 10% *trans*-configuration (Figure S7). The resulting PE(BiL<sup>O</sup>) is an amorphous material with a relatively high  $T_g$  of 154–158 °C, determined by differential scanning calorimetry (DSC) (Figure 1B and S10).

The structure of the resulting PE(BiL<sup>O</sup>) was further characterized by matrix-assisted laser desorption/ionization time-of-flight mass spectrometry (MALDI-TOF-MS), revealing a linear chain structure and high end-group fidelity (Figure 1C). Specifically, the BnOH-initiated linear structure, featuring only the anticipated end groups,  $\text{BnO}[\text{BiL}^{\text{O}}]_n\text{-H}$ , was confirmed by MALDI-TOF-MS using a low molar mass sample prepared with  $[\text{BiL}^{\text{O}}]/[\text{TBD}]/[\text{BnOH}]$  at a ratio of 100:1:1. The MS spectrum consisted of a single series of molecular ion peaks, with the spacing between neighboring molecular ion peaks corresponding to the exact molar mass of the repeat unit ( $m/z = 140.1$ ). This is demonstrated by the slope (140.1) of the linear plot of  $m/z$  values ( $y$ ) versus the number of BiL<sup>O</sup> repeat units ( $x$ ) (Figure S11). The intercept of the plot, 131.0, represents the total mass of chain ends and  $\text{Na}^+$  [ $108.1 (\text{BnO}/\text{H}) + 23.0 (\text{Na}^+) \text{ g mol}^{-1}$ ].

### Chemical Recycling of PE(BiL<sup>O</sup>) to Monomer BiL<sup>O</sup>

The depolymerization of PE(BiL<sup>O</sup>), produced from TBD, was initially investigated by solution depolymerization, utilizing 5 mol% TBD in toluene- $d_8$  (20 mg/mL). After heating at 120 °C for 12 h, the PE(BiL<sup>O</sup>) solid, which is insoluble in toluene, disappeared, and pure BiL<sup>O</sup> was regenerated, as confirmed by  $^1\text{H}$  NMR spectrum (Figure S12). Subsequently, we explored the bulk depolymerization of PE(BiL<sup>O</sup>) under vacuum using a sublimation apparatus, with superbases 1-tert-butyl-4,4,4-tris(dimethylamino)-2,2-bis[tris(dimethylamino)-phosphoranylid-enamino]-2 $\lambda^5,4\lambda^5$ -catenadi(phosphazene) (Bu-P<sub>4</sub>) as the catalyst (0.5 mol%) at 130 °C. PEG-2000 was employed as a matrix to ensure effective mixing of the polymer and catalyst.<sup>[20]</sup> Under these conditions, pure BiL<sup>O</sup> was recovered with a selectivity >99% and an isolated yield of 94% within 1 h. To quantify the thermodynamic parameters related to the chemical recycling of PE(BiL<sup>O</sup>), we conducted a variable-temperature NMR study with  $[\text{BiL}^{\text{O}}]/[\text{TBD}]/[\text{BnOH}] = 10/1/1$  and  $[\text{BiL}^{\text{O}}]_0 = 2.0 \text{ mol L}^{-1}$  in  $\text{CD}_2\text{Cl}_2$  from 35 °C to 5 °C in 10 °C increments. The equilibrium monomer concentrations,  $[\text{BiL}^{\text{O}}]_{\text{eq}}$ , were measured to be 1.57, 1.37, 1.18, and 0.97 mol L<sup>-1</sup> at temperatures of 35, 25, 15, and 5 °C, respectively. The van't Hoff plot of  $\ln[\text{BiL}^{\text{O}}]$  versus  $1000/T$  yielded a linear relationship ( $R^2 = 0.999$ ) (Figure S13). Application of the equation  $\ln[\text{BiL}^{\text{O}}]_{\text{eq}} = \Delta H_p^\circ/RT - \Delta S_p^\circ/R$  enabled extraction of the enthalpy and entropy of polymerization, with values determined to be  $\Delta H_p^\circ = -10.1 \text{ kJ mol}^{-1}$  and  $\Delta S_p^\circ = -36.5 \text{ J mol}^{-1} \text{ K}^{-1}$ . Assuming that these values are valid for all  $[\text{BiL}^{\text{O}}]_0$  conditions, the  $T_c$  was calculated to be 4 °C, when extrapolated to  $[\text{BiL}^{\text{O}}]_0 = 1.0 \text{ mol L}^{-1}$ , or 270 °C, when extrapolated to bulk state ( $[\text{BiL}^{\text{O}}]_0 \sim 8.6 \text{ mol L}^{-1}$ ), based on the equation  $T_c = \Delta H_p^\circ / \{\Delta S_p^\circ + R \ln[\text{BiL}^{\text{O}}]_0\}$ . Despite this low  $T_c$ , the resulting PE(BiL<sup>O</sup>) still exhibits good thermal stability with a decomposition temperature ( $T_{d,5\%}$ , the temperature at 5% weight loss) of 289 °C, as determined by thermogravimetric analysis (TGA) (Figure S14). This stability is attributable to the quenched or dead polymer chain being kinetically trapped.<sup>[1d]</sup>

The thermodynamic parameters of PE(BiL<sup>o</sup>) highlight a delicately balanced monomer-polymer equilibrium, which is critical for effective recycling while still ensuring viable polymerizability even at high BiL<sup>o</sup> concentrations. Impressively, catalyst-free bulk depolymerization under vacuum at 190 °C was successfully accomplished, delivering an isolated yield of 93 % with over 99 % selectivity (Figure 2). The observed full conversion of the PE(BiL<sup>o</sup>) with mixed (~1/1) *trans/cis*-configuration to the monomer BiL<sup>o</sup> with the fixed *cis*-configuration suggests that epimerization at the tertiary carbon (CH)  $\alpha$  to the ester carbonyl takes place under the depolymerization conditions. Whilst the  $T_c$  serves as an indicator of the static equilibrium between monomer and polymer state, depolymerization under vacuum conditions operates under a dynamic equilibrium. In this scenario, the continuous removal of newly generated monomers from the system circumvents the constraints typically imposed by  $T_c$ . A key consideration in implementing depolymerization under dynamic equilibrium conditions is the requirement for an external stimulus, such as heat or light, with or without a catalyst. This stimulus needs to surmount the energy barrier associated with depolymerization while concurrently preventing undesirable side reactions, such as decomposition.<sup>[1d,21]</sup>

### The Epoxide Manifold to Produce CO<sub>2</sub>-Based Polycarbonate PC(BiL<sup>o</sup>) via ROCOP

Following the successful establishment of closed-loop circularity for BiL<sup>o</sup> through its ROP pathway, we turned our attention to the epoxide manifold of the monomer. The

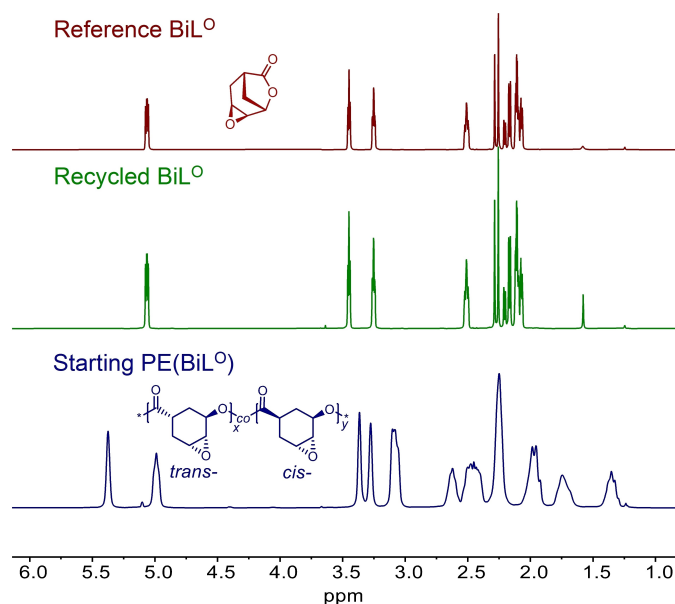


**Figure 2.** Stacked <sup>1</sup>H NMR (CDCl<sub>3</sub>) spectra of PE(BiL<sup>o</sup>) with 50% *trans*-configuration prepared by TBD with  $M_n = 11.4 \text{ kg mol}^{-1}$  and  $\bar{D} = 1.38$  (bottom); the recovered monomer BiL<sup>o</sup> obtained after depolymerization at 190 °C without catalyst under vacuum (middle); and the starting monomer BiL<sup>o</sup> for comparison (top).

homo-polymerization of the epoxide manifold was investigated using B(C<sub>6</sub>F<sub>5</sub>)<sub>3</sub> as the catalyst in CH<sub>2</sub>Cl<sub>2</sub> (5 M) at 23 °C with a [BiL<sup>o</sup>]/[B(C<sub>6</sub>F<sub>5</sub>)<sub>3</sub>] ratio of 100:1. Upon the addition of B(C<sub>6</sub>F<sub>5</sub>)<sub>3</sub> to the reaction solution, polymer precipitated out of the solution immediately. Subsequent attempts to dissolve the polymer in a variety of solvents, including DMF, DMSO, CHCl<sub>3</sub>, CH<sub>2</sub>Cl<sub>2</sub>, and 1,1,1,3,3,3-hexafluoro-2-propanol (HFIP), proved unsuccessful, suggesting the formation of a crosslinked polymer network. Thermal analysis of the crosslinked polymer revealed a high  $T_{d,5\%}$  of 336 °C and a  $T_g$  of 188 °C (Figure S15 and S16). The observed uncontrolled polymerization of the epoxide manifold may be a result of concurrent lactone ring-opening occurring during the epoxide polymerization process.<sup>[22]</sup>

To pursue the chemoselective polymerization of the epoxide manifold within BiL<sup>o</sup>, ROCOP of epoxide with CO<sub>2</sub> was explored, which was anticipated to produce PC(BiL<sup>o</sup>) featuring a bridged lactone in the repeat units. Initially, the ROCOP of BiL<sup>o</sup> with CO<sub>2</sub> was tested using commercially available Cr<sup>III</sup>-Salen/PPNCl [bis(triphenylphosphine)iminium chloride] catalyst system (Figure 3). The copolymerization was conducted in bulk at 130 °C and 40 bar CO<sub>2</sub>, with catalyst loadings ranging from 0.0125–1 mol % (Table 1; Figure S17 and S18). MALDI-TOF-MS analysis of a low molar mass PC(BiL<sup>o</sup>) sample confirmed the formation of carbonate repeat units, with the adjacent molecular ion peak spacing corresponding to the exact molar mass of the carbonate repeat unit ( $m/z = 184.1$ ) (Figure 4A). Additionally, Fourier Transform Infrared (FTIR) spectroscopy comparison between PE(BiL<sup>o</sup>) and PC(BiL<sup>o</sup>) revealed the appearance of a new C=O stretching frequency ( $\nu_{C=O}$ ) at 1802 cm<sup>-1</sup>, which corresponds to the carbonate group (Figure 4B). The resulting amorphous PC exhibited a relatively high  $T_g$  of 181 °C and a  $T_{d,5\%}$  of 298 °C (Figure 4C and 4D).

Manipulation of the [BiL<sup>o</sup>]/[PPNCl] ratio, whilst maintaining the [BiL<sup>o</sup>]/[Cr<sup>III</sup>-Salen] ratio, allowed for control over the  $M_n$  of PC(BiL<sup>o</sup>) (Table 1, runs 1–3). However, further increasing the [BiL<sup>o</sup>]:[Cr<sup>III</sup>-Salen]/[PPNCl] ratio did not yield a higher  $M_n$  PC (Table 1, runs 4–7), either due to

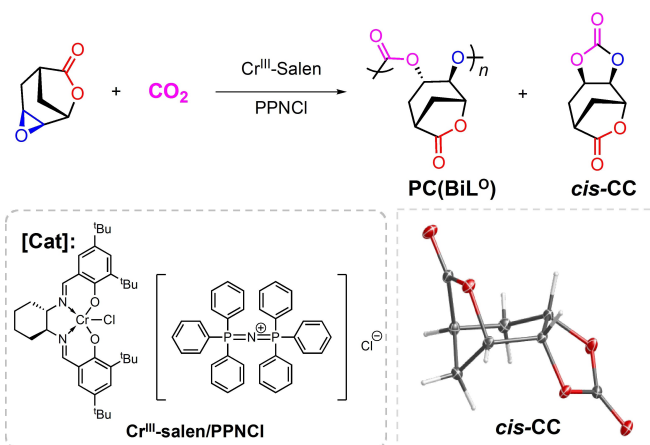


**Figure 3.** ROCOP of BiL<sup>o</sup> and CO<sub>2</sub>, catalyzed by a Cr<sup>III</sup>-Salen/PPNCl catalyst system.

**Table 1:** Results of ROCOP of BiL<sup>o</sup> with CO<sub>2</sub> catalyzed by Cr<sup>III</sup>-Salen and PPNCl.<sup>[a]</sup>

Run	[BiL <sup>o</sup> ]/[Cr <sup>III</sup> -Salen]/ [PPNCl]	Time (h)	Conv. <sup>[b]</sup> (%)	Selectivity <sup>[b]</sup> (polymer%)	M <sub>w</sub> <sup>[c]</sup> (kg mol <sup>-1</sup> )	M <sub>n</sub> <sup>[c]</sup> (kg mol <sup>-1</sup> )	Đ <sup>[c]</sup> (M <sub>w</sub> /M <sub>n</sub> )
1	100/1/1	8	99	65	109.1	23.3	4.7
2	100/1/2	8	99	65	33.0	8.5	3.9
3	100/1/0.5	8	99	67	158.2	42.7	3.7
4	250/1/1	8	99	59	121.0	28.3	4.3
5	500/1/1	24	99	64	172.9	38.5	4.5
6	1000/1/1	24	99	64	160.6	32.5	4.9
7	2000/1/1	48	94	62	119.6	21.7	5.5
8	250/1/0.5	24	98	67	113.6	25.9	4.4
9	500/1/0.5	24	99	64	133.6	32.6	4.1
10	1000/1/0.5	24	86	55	179.4	43.1	4.2

Conditions: [a] polymerization was conducted in bulk at 130 °C. [b] Monomer conversions were measured by <sup>1</sup>H NMR spectrum of the quenched solution in trifluoroacetic acid (TFA)-d<sub>1</sub>. [c] M<sub>w</sub>, M<sub>n</sub>, and Đ values determined by size-exclusion chromatography (SEC) at 40 °C in HFIP coupled with a DAWN HELEOS II multi (18)-angle light scattering detector and an Optilab TrEX dRI detector for absolute weight-average molar mass (M<sub>w</sub>).

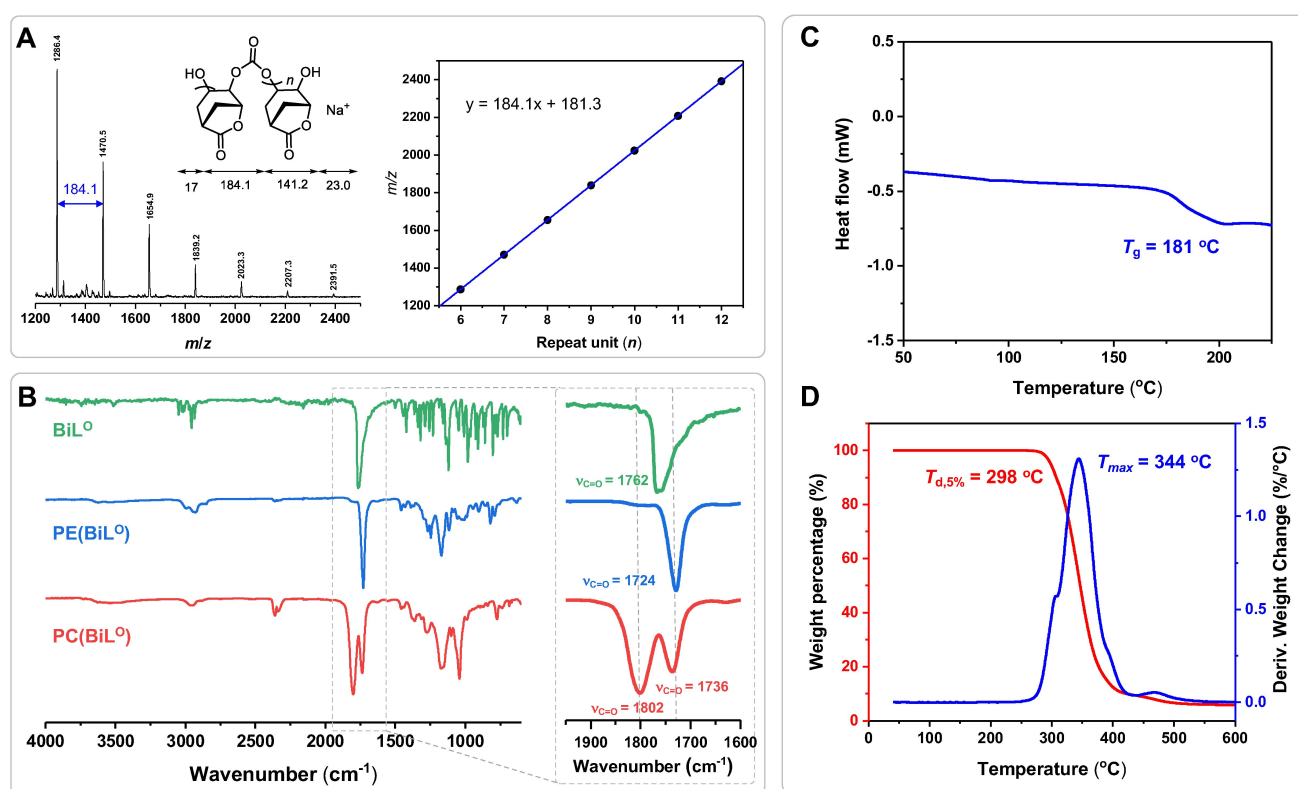


**Figure 4.** (A) MALDI-TOF MS spectrum and plot of mass/charge ratio (*m/z*) values versus the theoretical number of M repeat units for PC(BiL<sup>o</sup>) produced by Cr<sup>III</sup>-Salen and PPNCl. (B) FT-IR of PC(BiL<sup>o</sup>), PE(BiL<sup>o</sup>) and BiL<sup>o</sup>. (C) DSC curve for PC(BiL<sup>o</sup>). (D) TGA and DTG curves for PC(BiL<sup>o</sup>).

the occurrence of transcarbonation and carbonate back-biting side reactions, which is favored in the absence of Cr<sup>III</sup>-Salen, or the presence or residual water/alcohols in polymerization system limiting the obtained molar mass.<sup>[23]</sup> By fixing [Cr<sup>III</sup>-Salen]/[PPNCl] ratio at 2/1 and varying the [BiL<sup>o</sup>]/[Cr<sup>III</sup>-Salen] ratio, we achieved the highest M<sub>n</sub> of PC(BiL<sup>o</sup>), standing at 43.1 kg mol<sup>-1</sup> (Table 1, runs 8–10). However, the formation of *cis*-cyclic carbonate (*cis*-CC) byproduct, as confirmed via both NMR spectrum (Figure S20) and single-crystal structure analysis (Scheme 2, inset), limited the

polymer selectivity to 55–67%. Further efforts to optimize the polymerization conditions by manipulating parameters such as polymerization temperature, solvent, CO<sub>2</sub> pressure, and catalyst, did not completely suppress the formation of *cis*-CC; details are summarized in Table S2 and S3.

Chemical Recycling of PC(BiL<sup>o</sup>) to Monomer BiL<sup>o</sup>

Motivated by recent progress towards establishing “epoxide-polycarbonate” closed-loop circularity,<sup>[12–14]</sup> we investigated the depolymerization of the resulting PC(BiL<sup>o</sup>) to BiL<sup>o</sup>. Initially, we examined the thermolysis at 250 °C, employing a sublimation apparatus, given the solid nature of the monomer (Table 2, run 1). Unfortunately, this process predominantly resulted in the formation of *cis*-CC (60%), with only 18% conversion into BiL<sup>o</sup> and 22% of the unknown byproduct (Figure S21). The selectivity of BiL<sup>o</sup> was improved to 55%, with 45% *cis*-CC formed as the byproduct, by using 2.5 wt% (~0.5 mol%) of Cr<sup>III</sup>-Salen/PPNCl as the depolymerization catalyst at 150 °C for 5 h with PEG-2000 as the matrix (Table 2, run 2; Figure S21). Substituting PPNCl with PPNN<sub>3</sub> (bis(triphenylphosphine)iminium azide) dramatically improved the results, achieving a selectivity of BiL<sup>o</sup> formation >99% and a yield of 69% in 5 min (Table 2, run 3). By extending the depolymerization duration to 1 h after collecting the initially generated BiL<sup>o</sup>, we obtained an additional 7% sublimate, but a significant (43%) *cis*-CC impurity was observed (Table 2, run 4; Figure S22). This implies that the residual catalyst still showed reactivity for the depolymerization of further added PC(BiL<sup>o</sup>), but with much lower selectivity of 56% and a diminished depolymerization rate, which is similar to the results obtained with Cr<sup>III</sup>-Salen/PPNCl as the depolymerization catalyst. Nevertheless, when the PC was added in combination with 2.5 wt% PPNN<sub>3</sub>, it facilitated the clean and rapid recovery of BiL<sup>o</sup> with a quantitative selectivity of >99%.

It's worth highlighting that, in contrast to the outcomes observed with Cr<sup>III</sup>-Salen/PPNCl, we noticed the appearance of peaks in the aromatic region of <sup>1</sup>H NMR spectrum of the sublimate during the late stages of depolymerization catalyzed by Cr<sup>III</sup>-Salen/PPNN<sub>3</sub>. We attribute these peaks to the potential decomposition of PPNN<sub>3</sub>, an assumption supported by the bubbles observed during the depolymerization process and the emergence of analogous peaks when PPNN<sub>3</sub> was heated at 160 °C in the absence of the PC (Figure S23).

These results suggest that the critical role of PPNN<sub>3</sub> in facilitating the rapid and selective depolymerization of the PC. And the decomposition of PPNN<sub>3</sub>, particularly the azide anion, seems to contribute to decreased selectivity and slower depolymerization rates during the latter stages of depolymerization. Lu and co-workers have reported a similar decomposition phenomenon during PCHC recycling catalyzed by Cr<sup>III</sup>-Salen/PPNN<sub>3</sub>, where recycling selectivity dropped from 99% to 97% during the second depolymerization cycle, echoing our findings with Cr<sup>III</sup>-Salen/PPNCl. Accordingly, we implemented a strategy to suppress the formation of *cis*-CC byproduct by introducing an additional 2.5 wt% PPNN<sub>3</sub> into the reaction system midway through the depolymerization reaction. Following optimization of the experimental conditions, we were able to achieve depolymerization with an improved yield of 91% and good selectivity (~94%) when applying a temperature of 180 °C for 10 min (Table 2, run 7). The high turnover frequency (TOF) of up to 1300 h<sup>-1</sup> further attests to the high efficiency of the depolymerization process in recovering the epoxide monomer. The OH present in PEG-2000 may trigger scission of PC(BiL<sup>o</sup>), thus facilitating the depolymerization.

This intriguing finding prompted us to further investigate the underlying origins of the improved selectivity observed with the N<sub>3</sub><sup>-</sup> anion compared with Cl<sup>-</sup>. A plausible explanation could lie in the increased nucleophilicity and/or basicity of N<sub>3</sub><sup>-</sup>, which may facilitate the deprotonation of the polymer chain end –OH and promote the selective formation of BiL<sup>o</sup> through catalyzed alkoxide back-biting, while simultaneously minimizing the formation of the undesired *cis*-CC through carbonate back-biting.<sup>[10,23a]</sup> With this hypothesis in mind, organic superbases <sup>t</sup>Bu-P<sub>4</sub> was subsequently tested as the catalyst (0.7 mol%) for the depolymerization of the PC at 160 °C (Table 2, run 8). Under these conditions, BiL<sup>o</sup> was recovered in 89% yield in 30 min, with a >99% selectivity and a TOF of 254 h<sup>-1</sup>. However, the high basicity of <sup>t</sup>Bu-P<sub>4</sub> may result in the chain scission of the matrix PEG-2000, potentially leading to trace contamination of the recovered BiL<sup>o</sup> with PEG oligomers. A simple base KOMe was also found to be effective in catalyzing the depolymeri-

**Table 2:** Results of depolymerization of PC(BiL<sup>o</sup>) catalyzed by various catalysts.<sup>[a]</sup>

Run	[Cat]/[Cocat]	Temp. (°C)	Time (min)	Yield <sup>[b]</sup> (%)	TOF <sup>[c]</sup> (h <sup>-1</sup> )	Selectivity <sup>[d]</sup> (%)		byproduct
						BiL <sup>o</sup>	<i>cis</i> -CC	
1	–/–	250	30	–	–	18	60	22
2	Cr <sup>III</sup> -Salen/PPNCl (2.5 wt%)	150	300	–	–	55	45	–
3	Cr <sup>III</sup> -Salen/PPNN <sub>3</sub> (2.5 wt%)	160	5	69	1183	>99	–	–
4	Cr <sup>III</sup> -Salen/PPNN <sub>3</sub> (2.5 wt%)	160	65	76	113	96	4	–
5	Cr <sup>III</sup> -Salen/PPNN <sub>3</sub> (2.5 wt%)	130	20	18	71	92	8	–
6	Cr <sup>III</sup> -Salen/PPNN <sub>3</sub> (2.5 wt%)	230	5	84	1296	90	10	–
7	Cr <sup>III</sup> -Salen/PPNN <sub>3</sub> (2.5 wt%)	180	10	91	733	94	6	–
8	<sup>t</sup> Bu-P <sub>4</sub> /– (2.5 wt%)	160	30	89	254	>99	–	–
9	KOMe/– (10 wt%)	160	120	73	6	>99	–	–
10	TBD/MSA = 1/1 (5 wt%)	160	15	79	–	23	77	–
11	TBD/TfOH = 1/1 (5 wt%)	160	15	87	–	–	>99	–

Conditions: [a] Depolymerization conducted in sublimation apparatus under vacuum, the [Cat] and [Cocat] were added at 1:1 ratio, wt% was determined by the mass of added [Cat] to the PC(BiL<sup>o</sup>) mass. [b] Yield determined by the recovery mass. [c] Turnover frequency (TOF) = (mol of recovered BiL<sup>o</sup>)/(mol of [Cat] \* hour). [d] Selectivity measured by <sup>1</sup>H NMR spectrum of the quenched solution in TFA-d<sub>1</sub>.

zation of PC(BiL<sup>o</sup>) into BiL<sup>o</sup> with a selectivity of over 99 %, under the guidance of the proposed selective depolymerization mechanism, although it did exhibit lower activity (Table 2, run 9). In comparison to that observed for PCHC depolymerization, only *cis*-CC, rather than *trans*-CC, was observed in both the polymerization and depolymerization processes of BiL<sup>o</sup>. We attribute this phenomenon to the introduction of the bridged ester bond in the monomer structure, which significantly alters the configuration of the bicyclic cyclohexane, rendering the formation of *trans*-CC thermodynamically unstable, aligning with poly(cyclopentene carbonate) scenario.<sup>[9d,23a, 24]</sup> Overall, we propose that the basic catalysts applied promote ionization at the polymer hydroxyl chain-end, resulting in a highly nucleophilic alkoxide which, in turn, facilitates the production of the epoxy-containing monomer BiL<sup>o</sup> (Figure 5B). To further probe our hypothesis, we investigated the use of a protic ionic salt catalyst, TBD: Methanesulfonic acid (MSA)=1/1 (Figure 5A). Consistent with catalyst basicity playing a key role in determining selectivity, use of this catalyst resulted in a BiL<sup>o</sup> selectivity of just 23 % (Table 2, run 10). Replacing MSA with stronger Brønsted acid TfOH, the protic ionic salt TBD: TfOH=1/1 afforded almost exclusively in the production of *cis*-CC as a depolymerization product (Table 2, run 11, Figure S24). We hypothesize that this is due to Lewis acid stabilization of the carbonate chain-end, which inhibited CO<sub>2</sub> release and thus resulted in *cis*-CC becoming the exclusive product.

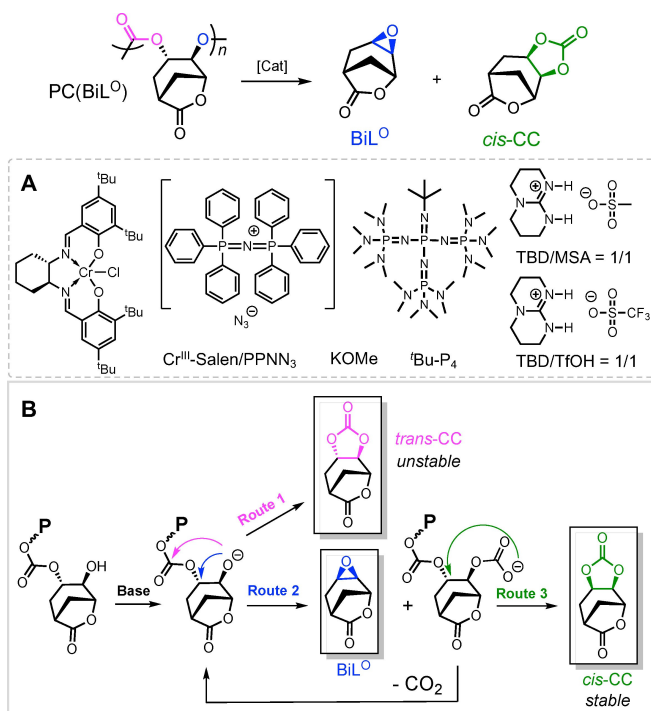


**Figure 5.** (A) Catalysts for selective depolymerization of PC(BiL<sup>o</sup>) to BiL<sup>o</sup> and CO<sub>2</sub> or *cis*-CC. (B) The proposed depolymerization mechanism of PC(BiL<sup>o</sup>): Depolymerization products only consist of BiL<sup>o</sup> produced from alkoxide backbiting and *cis*-CC produced from carbonate backbiting, with *trans*-CC being too thermodynamically unstable to form.

### Closed-Loop Recycling of Plastics Mixture to Monomer BiL<sup>o</sup>

Given that tBu-P<sub>4</sub> had demonstrated remarkable activity in the depolymerization of both PC(BiL<sup>o</sup>) and PE(BiL<sup>o</sup>) to reform monomer BiL<sup>o</sup>, we postulated that tBu-P<sub>4</sub> could also serve as an optimal catalyst for the depolymerization of a plastics mixture consisting of PC(BiL<sup>o</sup>) and PE(BiL<sup>o</sup>). A 1:1 PC(BiL<sup>o</sup>)/PE(BiL<sup>o</sup>) mixture served as a representative sample to assess the efficacy and performance of the depolymerization process catalyzed by tBu-P<sub>4</sub>. Specifically, the PC(BiL<sup>o</sup>)/PE(BiL<sup>o</sup>) mixture was placed in the sublimation apparatus, along with 2 grams of PEG-2000 serving as a matrix. Following the addition of tBu-P<sub>4</sub> (at 1 mol %), a vacuum was applied within the sublimation apparatus and started the depolymerization process at 150 °C. The mixed plastics were effectively depolymerized back to their single constituent monomer BiL<sup>o</sup> in 86 % isolated yield with >99 % selectivity in 25 min (Figures S25 and S26), hence demonstrating a rare example of one-pot recycling of mixed plastics.

### Conclusions

We present here an advancement in developing effective approach to address the challenging goal of closed-loop recycling of EoL mixed plastics through design of multifunctional monomers that can lead to multiple polymers of different classes and performance properties, through orthogonal polymerization. The resulting diverse polymers and their mixtures all can be chemically recycled back to their single-source, original monomer in exclusive selectivity and high recovery yield, without the requiring prior sorting or separation. Specifically, our design of bifunctional lactone/epoxide monomer BiL<sup>o</sup> that undergoes orthogonal polymerization into lactone-based polyester PE(BiL<sup>o</sup>) and CO<sub>2</sub>-based polycarbonate PC(BiL<sup>o</sup>). Importantly, both homopolymers, PE(BiL<sup>o</sup>) and PC(BiL<sup>o</sup>), and their mixture can all be depolymerized back to the original monomer in quantitative (>99 %) selectivity in the presence of the same catalyst at 150 °C. Furthermore, our exploration of the “epoxide-polycarbonate” closed-loop circularity has shed additional light on the integral role of catalysts and the monomer structure on depolymerization behaviors. While there is still room for further improvement in aspects such as polymerization selectivity and the depolymerization efficiency, this work continues to create new solutions for tackling the longstanding challenge of mixed plastic recycling and underscores the critical importance of strategic monomer design in advancing sustainable solutions in polymer science. Lastly, the functional groups of the epoxide still present in PE(BiL<sup>o</sup>) and the lactone still present in PC(BiL<sup>o</sup>) could potentially be utilized for post-functionalization via curing or copolymerization to produce additional high-performance materials; the work directed at this direction is underway.

## Acknowledgements

We gratefully acknowledge support by the U.S. Department of Energy, Office of Energy Efficiency and Renewable Energy, Advanced Materials and Manufacturing Technologies Office (AMMTO) and Bioenergy Technologies Office (BETO). This work was performed as part of the Bio-Optimized Technologies to keep Thermoplastics out of Landfills and the Environment (BOTTLE) Consortium and was supported by AMMTO and BETO under Contract DE-AC36-08GO28308 with the National Renewable Energy Laboratory (NREL), operated by Alliance for Sustainable Energy, LLC. The BOTTLE Consortium includes members from Colorado State University (CSU). We thank C. Lincoln and J. Miscall of NREL for SEC analysis of that polymer samples that need HFIP to solubilize them, and Dr. Z. Zhang of CSU for help with some experiments for revisions.

## Conflict of Interest

The authors declare no conflict of interest.

## Data Availability Statement

The Supporting Information for this manuscript is available as a PDF. Deposition Numbers 2262281 (for BiL<sup>0</sup>) and 2262280 (for cis-CC) contain the supplementary crystallographic data for this paper. These data are provided free of charge by the joint Cambridge Crystallographic Data Centre and Fachinformationszentrum Karlsruhe Access Structures service.

**Keywords:** Chemically recyclable polymer · Mixed plastics recycling · Orthogonal (de)polymerization · Polyester · CO<sub>2</sub>-polycarbonate

- [1] a) C. Shi, L. T. Reilly, E. Y.-X. Chen, *Angew. Chem. Int. Ed.* **2023**, *62*, e202301850; b) Y. Liu, X.-B. Lu, *Chem. Eur. J.* **2023**, *29*, e202203635; c) G. Xu, Q. Wang, *Green Chem.* **2022**, *24*, 2321–2346; d) C. Shi, L. T. Reilly, V. S. Phani Kumar, M. W. Coile, S. R. Nicholson, L. J. Broadbelt, G. T. Beckham, E. Y. X. Chen, *Chem* **2021**, *7*, 2896–2912; e) G. W. Coates, Y. D. Y. L. Getzler, *Nat. Rev. Mater.* **2020**, *5*, 501–516; f) X. Tang, E. Y. X. Chen, *Chem* **2019**, *5*, 284–312; g) M. Hong, E. Y. X. Chen, *Trends Chem.* **2019**, *1*, 148–151; h) X.-B. Lu, Y. Liu, H. Zhou, *Chem. Eur. J.* **2018**, *24*, 11255–11266; i) A. Rahimi, J. M. Garcia, *Nat. Chem. Rev.* **2017**, *1*, 0046; j) M. Hong, E. Y. X. Chen, *Green Chem.* **2017**, *19*, 3692–3706; k) F. M. Haque, J. S. A. Ishibashi, C. A. L. Lidston, H. Shao, F. S. Bates, A. B. Chang, G. W. Coates, C. J. Cramer, P. J. Dauenhauer, W. R. Dichtel, C. J. Ellison, E. A. Gormong, L. S. Hamachi, T. R. Hoye, M. Jin, J. A. Kalow, H. J. Kim, G. Kumar, C. J. LaSalle, S. Liffland, B. M. Lipinski, Y. Pang, R. Parveen, X. Peng, Y. Popowski, E. A. Prebhalo, Y. Reddi, T. M. Reineke, D. T. Sheppard, J. L. Swartz, W. B. Tolman, B. Vlaisavljevich, J. Wissinger, S. Xu, M. A. Hillmyer, *Chem. Rev.* **2022**, *122*, 6322–6373.
- [2] a) I. Vollmer, M. J. F. Jenks, M. C. P. Roelands, R. J. White, T. van Harmelen, P. de Wild, G. P. van der Laan, F. Meirer, J. T. F. Keurentjes, B. M. Weckhuysen, *Angew. Chem. Int. Ed.* **2020**, *59*, 15402–15423; b) Z. O. G. Schyns, M. P. Shaver, *Macromol. Rapid Commun.* **2021**, *42*, 2000415; c) J. Maris, S. Bourdon, J.-M. Brossard, L. Cauret, L. Fontaine, V. Montembault, *Polym. Degrad. Stab.* **2018**, *147*, 245–266; d) J. Zhou, T.-G. Hsu, J. Wang, *Angew. Chem. Int. Ed.* **2023**, *62*, e202300768.
- [3] a) M. Hong, E. Y. X. Chen, *Nat. Chem.* **2016**, *8*, 42–49; b) X. Tang, M. Hong, L. Falivene, L. Caporaso, L. Cavallo, E. Y. X. Chen, *J. Am. Chem. Soc.* **2016**, *138*, 14326–14337; c) J.-B. Zhu, E. M. Watson, J. Tang, E. Y.-X. Chen, *Science* **2018**, *360*, 398–403; d) B. A. Abel, R. L. Snyder, G. W. Coates, *Science* **2021**, *373*, 783–789; e) M. Häußler, M. Eck, D. Rothauer, S. Mecking, *Nature* **2021**, *590*, 423–427; f) L. Zhou, Z. Zhang, C. Shi, M. Scotti, D. K. Barange, R. R. Gowda, E. Y.-X. Chen, *Science* **2023**, *380*, 64–69; g) T. M. McGuire, A. Buchard, C. Williams, *J. Am. Chem. Soc.* **2023**; h) L. Cederholm, J. Wohler, P. Olsén, M. Hakkarainen, K. Odellius, *Angew. Chem. Int. Ed.* **2022**, *61*; i) Y. Wang, Y. Zhu, W. Lv, X. Wang, Y. Tao, *J. Am. Chem. Soc.* **2023**, *145*, 1877–1885; j) J. D. Feist, Y. Xia, *J. Am. Chem. Soc.* **2020**, *142*, 1186–1189; k) D. Sathe, J. Zhou, H. Chen, H.-W. Su, W. Xie, T.-G. Hsu, B. R. Schrage, T. Smith, C. J. Ziegler, J. Wang, *Nat. Chem.* **2021**, *13*, 743–750; l) J. Yuan, W. Xiong, X. Zhou, Y. Zhang, D. Shi, Z. Li, H. Lu, *J. Am. Chem. Soc.* **2019**, *141*, 4928–4935.
- [4] a) R. W. Clarke, T. Sandmeier, K. A. Franklin, D. Reich, X. Zhang, N. Vengallur, T. K. Patra, R. J. Tannenbaum, S. Adhikari, S. K. Kumar, T. Rovis, E. Y. X. Chen, *Nature* **2023**, *616*, 731–739; b) J. M. Eagan, J. Xu, R. Di Girolamo, C. M. Thurber, C. W. Macosko, A. M. LaPointe, F. S. Bates, G. W. Coates, *Science* **2017**, *355*, 814–816.
- [5] a) K. P. Sullivan, A. Z. Werner, K. J. Ramirez, L. D. Ellis, J. R. Bussard, B. A. Black, D. G. Brandner, F. Bratti, B. L. Buss, X. Dong, S. J. Haugen, M. A. Ingraham, M. O. Konev, W. E. Michener, J. Miscall, I. Pardo, S. P. Woodworth, A. M. Guss, Y. Román-Leshkov, S. S. Stahl, G. T. Beckham, *Science* **2022**, *378*, 207–211; b) B. D. Vogt, K. K. Stokes, S. K. Kumar, *ACS Appl. Polym. Mater.* **2021**, *3*, 4325–4346.
- [6] a) M.-Q. Zhang, M. Wang, B. Sun, C. Hu, D. Xiao, D. Ma, *Chem* **2022**, *8*, 2912–2923; b) L. T. J. Korley, T. H. Epps, B. A. Helms, A. J. Ryan, *Science* **2021**, *373*, 66–69; c) A. Arroyave, S. Cui, J. C. Lopez, A. L. Kocen, A. M. LaPointe, M. Delferro, G. W. Coates, *J. Am. Chem. Soc.* **2022**, *144*, 23280–23285; d) F. Zhang, M. Zeng, R. D. Yappert, J. Sun, Y.-H. Lee, A. M. LaPointe, B. Peters, M. M. Abu-Omar, S. L. Scott, *Science* **2020**, *370*, 437–441; e) C. Jehanno, J. W. Alty, M. Roosen, S. De Meester, A. P. Dove, E. Y. X. Chen, F. A. Leibfarth, H. Sardon, *Nature* **2022**, *603*, 803–814; f) R. J. Conk, S. Hanna, J. X. Shi, J. Yang, N. R. Ciccio, L. Qi, B. J. Bloomer, S. Heuvel, T. Wills, J. Su, A. T. Bell, J. F. Hartwig, *Science* **2022**, *377*, 1561–1566.
- [7] a) S. Dabral, T. Schaub, *Adv. Synth. Catal.* **2019**, *361*, 223–246; b) M. Aresta, A. Dibenedetto, A. Angelini, *Chem. Rev.* **2014**, *114*, 1709–1742; c) J. Artz, T. E. Müller, K. Thenert, J. Kleinekorte, R. Meys, A. Sternberg, A. Bardow, W. Leitner, *Chem. Rev.* **2018**, *118*, 434–504.
- [8] a) D. J. Darensbourg, *Chem. Rev.* **2007**, *107*, 2388–2410; b) X.-B. Lu, W.-M. Ren, G.-P. Wu, *Acc. Chem. Res.* **2012**, *45*, 1721–1735; c) M. I. Childers, J. M. Longo, N. J. Van Zee, A. M. LaPointe, G. W. Coates, *Chem. Rev.* **2014**, *114*, 8129–8152; d) J. Huang, J. C. Worch, A. P. Dove, O. Coulembier, *ChemSusChem* **2020**, *13*, 469–487; e) S. Tang, K. Nozaki, *Acc. Chem. Res.* **2022**, *55*, 1524–1532; f) Y. Liu, X.-B. Lu, *Macromolecules* **2023**, *56*, 1759–1777.
- [9] a) Y. Liu, H. Zhou, J.-Z. Guo, W.-M. Ren, X.-B. Lu, *Angew. Chem. Int. Ed.* **2017**, *56*, 4862–4866; b) C. Li, R. J. Sablong,

- R. A. T. M. van Benthem, C. E. Koning, *ACS Macro Lett.* **2017**, *6*, 684–688; c) Y. Yu, L.-M. Fang, Y. Liu, X.-B. Lu, *ACS Catal.* **2021**, *11*, 8349–8357; d) G.-W. Yang, Y. Wang, H. Qi, Y.-Y. Zhang, X.-F. Zhu, C. Lu, L. Yang, G.-P. Wu, *Angew. Chem. Int. Ed.* **2022**, *61*, e202210243.
- [10] D. J. Darensbourg, S.-H. Wei, *Macromolecules* **2012**, *45*, 5916–5922.
- [11] D. J. Darensbourg, A. D. Yeung, S.-H. Wei, *Green Chem.* **2013**, *15*, 1578–1583.
- [12] a) F. N. Singer, A. C. Deacy, T. M. McGuire, C. K. Williams, A. Buchard, *Angew. Chem. Int. Ed.* **2022**, *61*, e202201785; b) X. Liao, F.-C. Cui, J.-H. He, W.-M. Ren, X.-B. Lu, Y.-T. Zhang, *Chem. Sci.* **2022**, *13*, 6283–6290.
- [13] Y. Yu, B. Gao, Y. Liu, X.-B. Lu, *Angew. Chem. Int. Ed.* **2022**, *61*, e202204492.
- [14] T. M. McGuire, A. C. Deacy, A. Buchard, C. K. Williams, *J. Am. Chem. Soc.* **2022**, *144*, 18444–18449.
- [15] E. C. Quinn, K. M. Knauer, G. T. Beckham, E. Y. X. Chen, *One Earth* **2023**, *6*, 582–586.
- [16] Y. Zhao, E. M. Rettner, K. L. Harry, Z. Hu, J. Miscall, N. A. Rorrer, G. M. Miyake, *Science* **2023**, *382*, 310–314.
- [17] a) C. Shi, M. L. McGraw, Z.-C. Li, L. Cavallo, L. Falivene, E. Y.-X. Chen, *Sci. Adv.* **2020**, *6*, eabc0495; b) C. Shi, Z.-C. Li, L. Caporaso, L. Cavallo, L. Falivene, E. Y. X. Chen, *Chem* **2021**, *7*, 670–685; c) R. M. Cywar, N. A. Rorrer, H. B. Mayes, A. K. Maurya, C. J. Tassone, G. T. Beckham, E. Y. X. Chen, *J. Am. Chem. Soc.* **2022**, *144*, 5366–5376; d) C. Shi, R. W. Clarke, M. L. McGraw, E. Y. X. Chen, *J. Am. Chem. Soc.* **2022**, *144*, 2264–2275; e) C. Shi, Z. Zhang, M. Scoti, X.-Y. Yan, E. Y.-X. Chen, *ChemSusChem* **2023**, *16*, e202300008.
- [18] D. Askin, C. Angst, S. Danishefsky, *J. Org. Chem.* **1985**, *50*, 5005–5007.
- [19] a) R. C. Pratt, B. G. G. Lohmeijer, D. A. Long, R. M. Waymouth, J. L. Hedrick, *J. Am. Chem. Soc.* **2006**, *128*, 4556–4557; b) A. Chuma, H. W. Horn, W. C. Swope, R. C. Pratt, L. Zhang, B. G. G. Lohmeijer, C. G. Wade, R. M. Waymouth, J. L. Hedrick, J. E. Rice, *J. Am. Chem. Soc.* **2008**, *130*, 6749–6754.
- [20] a) L.-G. Li, Q.-Y. Wang, Q.-Y. Zheng, F.-S. Du, Z.-C. Li, *Macromolecules* **2021**, *54*, 6745–6752; b) C. F. Gallin, W. W. Lee, J. A. Byers, *Angew. Chem. Int. Ed. Engl.* **2023**, e202303762.
- [21] a) G. R. Jones, H. S. Wang, K. Parkatzidis, R. Whitfield, N. P. Truong, A. Anastasaki, *J. Am. Chem. Soc.* **2023**, *145*, 9898–9915; b) V. Lohmann, G. R. Jones, N. P. Truong, A. Anastasaki, *Chem. Sci.* **2024**; c) A. Duda, A. Kowalski, in *Handbook of Ring-Opening Polymerization*, **2009**, pp. 1–51.
- [22] N. J. Van Zee, G. W. Coates, *Chem. Commun. (Camb.)* **2014**, *50*, 6322–6325.
- [23] a) D. J. Darensbourg, *Polym. Degrad. Stab.* **2018**, *149*, 45–51; b) W. T. Diment, C. K. Williams, *Chem. Sci.* **2022**, *13*, 8543–8549.
- [24] D. J. Darensbourg, S.-H. Wei, A. D. Yeung, W. C. Ellis, *Macromolecules* **2013**, *46*, 5850–5855.

Manuscript received: March 14, 2024

Accepted manuscript online: June 4, 2024

Version of record online: July 23, 2024